Band alignment of HfAlO/GaN (0001) determined by x-ray photoelectron spectroscopy: Effect of *in situ* SiH_4 Passivation

Xinke Liu[1], Zhihong Liu[2], Pannirselvam S/O Somasuntharam[2], Pan Jishen[3], Wei Liu[4], Fang Jia[1], Youming Lu[1*], Wenjie Yu[5*], and Leng Seow Tan[2]

[1]College of Material Science and Engineering, Shenzhen Key Laboratory of Special Functional Materials, Shenzhen University, People Republic of China, 518060

[2]Department of Electrical and Computer Engineering, National University of Singapore, Singapore, 117576

[3]Institute of Materials Research and Engineering, Agency for Science Technology and Research, Singapore, 117602

[4]Luminous! Centre of Excellence for Semiconductor Lighting and Displays, Nanyang Technological University, Singapore, 639785

[5]State Key Laboratory of Functional Materials for Informatics, Shanghai Institute of Microsystem and Information Technology, CAS, People Republic of China, 200050

Abstract

The energy band alignment between HfAlO and GaN (0001) was characterized using high-resolution x-ray photoelectron spectroscopy (XPS). The HfAlO was deposited using a metal-organic chemical vapor deposition (MOCVD) gate cluster. A valence band offset of 0.38 eV and a conduction band offset of 2.22 eV were obtained across the HfAlO/GaN heterointerface without any passivation. With *in situ* SiH_4 passivation (vacuum anneal+SiH_4 treatment) on the GaN surface right before HfAlO deposition, the valence band offset and the conduction band offset across the HfAlO/GaN heterointerface were found to be 0.51 eV and 2.09 eV, respectively. The difference in the band alignment is believed to be dominated by the core level up-shift or chemical shift in the GaN substrate as a result of different interlayers (ILs) formed by the two surface preparations.

Key words: Gallium nitride; high-*k*; band alignment; x-ray photoelectron spectroscopy.

1. Introduction

AlGaN/GaN high-electron-mobility transistor (HEMTs) are attractive for high power, high temperature, and high frequency applications, mainly due to the large critical electric field and high electron saturation velocity ($2.5x10^7$cm/s) of AlGaN/GaN heterostructure.[1-4] Although microwave output power density up to 32 W/mm and total RF output powers in excess of 360 W have been demonstrated, the issues related to the reliabilities faced by AlGaN/GaN HEMTs still remain to be solved in order to move toward commercially available devices.[5-6] As well know, the effect that most severely limits the RF power performance of AlGaN/GaN HEMTs is the so-called RF current collapse or RF power slump, which originates from trapping effects at the device surface and/or in the buffer.[7] One of the technological solutions that have been proposed as a possible cure for this detrimental effect is to passivate the surface using a dielectric, such as SiN_x, SiO_2, Al_2O_3, ZnO, etc.[5,8,9,10] In addition, AlGaN/GaN HEMTs with a conventional Schottky gate structure usually suffer from a large gate leakage, which reduces the maximum output power and results in some reliability issues.[11-12] High gate leakage could be reduced by integrating an oxide between the metal gate and the nitride and forming a metal-oxide-semiconductor (MOS) structure. The gate oxide layer also works as a surface passivation layer so as to reduce the surface traps and suppress the surface trapping effects. Various oxides have been investigated as the gate insulators in the MOSHEMTs, such as Al_2O_3, HfO_2, MgO, Sc_2O_3, ZrO_2 etc.[13-21] Among these dielectric materials, HfAlO is one of the most promising dielectrics to be applied into MOS-HEMTs, due to its higher crystallization temperature (~ 800 ºC) than that of pure HfO_2 (~ 400 ºC) and its higher dielectric constant (ε_r ~ 20) than that of pure Al_2O_3 (ε_r ~

9).[22-24]

Typically, people are using a thin GaN cap in the AlGaN/GaN HEMT or MOS-HEMT structures, in order to increase the Schottky barrier height and reduce the gate leakage current.[11-12] To understand the electrical properties of dielectric/nitride interface knowing its band alignment is very important. Band alignment at the dielectric/GaN interface would be very useful in the modeling of the gate leakage current and help in the design of AlGaN/GaN MOS-HEMTs with a GaN cap for optimum performance. There are some reports available on the band-alignment study for the Al_2O_3/GaN and HfO_2/GaN heterostructures.[25] However, still very few publications on the HfAlO/GaN band-alignment study can be found. Recent work showed that the AlGaN/GaN MOS-HEMTs with *in situ* SiH_4 passivation have an improved sub-threshold swing, an increased on-state current, and a reduced gate leakage current.[26-27] However, the effect of *in situ* SiH_4 passivation on the band alignment at HfAlO/GaN interface have not be fully investigated. As such, a study of the band alignment and effect of *in situ* SiH_4 passivation on HfAlO/GaN interface would be of interest, since the nature of this interface has a direct bearing on the device characteristics.

2. Experiment details

The band alignment at HfAlO/GaN interface was studied experimentally using x-ray photoelectron spectroscopy (XPS) for different surface treatments of GaN. The test samples were prepared using undoped GaN (0001) on sapphire wafers, and the GaN epitaxial layer has a thickness of 2 μm and a root-mean-square surface roughness of less than 0.5 nm. All samples went through the pre-gate cleaning process, which consisted of a 2-minute acetone, 3-minute isopropanol degreasing step, a 10-minute HCl (H_2O:

HCl=1:1) native oxide removal step, and an *ex situ* surface passivation using $(NH_4)_2S$ solution for 30 minutes. Work related to $(NH_4)_2S$ solution treatment could be found in Ref. [27]. After pre-gate cleaning, the wafers were quickly loaded into a multiple-chamber metal-organic chemical vapor deposition (MOCVD) gate cluster system for *in situ* SiH_4 passivation and high-*k* deposition. Vacuum anneal (VA) and SiH_4 treatment were performed for 1 minute under 300 and 400 ºC, respectively. The detailed process conditions of *in situ* SiH_4 passivation can be founded elsewhere.[28] After passivation, a 3 nm HfAlO high-*k* dielectric was deposited using the same MOCVD gate cluster. Before the dielectric deposition, the sample was not exposed to air ambient at all. Finally, there was a post-deposition anneal (PDA) at 500 ºC for 60 s in N_2 ambient for all the samples. For the control HfAlO(3nm)/GaN sample, VA and SiH_4 treatment were skipped. The "bulk samples" consist of a pre-cleaned GaN substrate and a HfAlO(30nm)/GaN substrate.

3. Results and discussion

Figure 1 shows the transmission electron microscopy (TEM) images of both the control and SiH_4 passivated samples. An interfacial layer (IL) of about 1 nm is observed in both samples. The nature of these layers formed by two different surface treatments was further investigated by XPS. In this experiment, XPS analysis was conducted using a mono-chromatized Al Kα (1486.6 Ev) x-ray source on the VG ESCALAB 220i-XL system with a constant pass energy of 20 eV. The banding energy calibration was performed using gold (Au), silver (Ag), and copper (Cu) standard samples by setting the Au $4f_{7/2}$, Ag $3d_{5/2}$, and Cu $2p_{3/2}$ peaks at binding energies of 83.98±0.02, 368.26±0.02,

and 932.67±0.02 eV, respectively. The Fermi level edge was calibrated using pure nickel (Ni) and setting the binding energy at 0.00±0.02 eV. To determine the valence band offset for the HfAlO/GaN interface, the Ga 3p and the Hf 4f core-level spectra were used for the GaN and HfAlO samples, respectively.

Figure 2 shows the XPS measurement for the core-level spectra as well as the valence band maximum (VBM) for the various samples. For the bulk samples, the VBM is obtained from the intercept of the slope at the leading edge of the valence band spectrum with the base line as shown in Figure 2 (a) and (b). XPS is well-established to determine the band discontinuities at the heterojunction interface, based on the assumption that the energy difference between the valence band edge and core level peak of the substrate is intact with or without the over-layer deposition.[29-31] Although the valence band offset at the interface of two materials can be estimated from the difference between VBMs, this contains an appreciable error since the interface dipole which generally exists is not accounted for. A more accurate value for the valence band offset ΔE_V between HfAlO and GaN can be obtained through the method discussed in Ref. 32 and is given by

$$\Delta E_V = (E_{CL,GaN} - E_{V,GaN}) - \Delta E_{CL} - (E_{CL,HfAlO} - E_{V,HfAlO}), \quad (1)$$

where $E_{CL,GaN}$ and $E_{V,GaN}$ are the core-level and the valence band maximum binding energy of the GaN bulk sample, $E_{CL,HfAlO}$ and $E_{V, HfAlO}$ are the core-level and the valence band maximum binding energy of the HfAlO bulk sample, and ΔE_{CL} is the difference between the respective core-level binding energy of HfAlO and GaN in the HfAlO/GaN interface sample.[33-35] Similar approach has been used to study the band alignment of GaN-related system, and can be found in Ref. [36]-[38]. The energy differences for the

bracketed terms as well as ΔE_{CL} are also illustrated in Figure 2. The valence band offset between the HfAlO and GaN as calculated from Ga 3p and the Hf 4f core-levels using Eq. (1) is 0.38 eV for the control sample. Based on the valence band offset, the conduction band offset can be calculated by

$$\Delta E_C = E_{G,HfAlO} - E_{G,GaN} - \Delta E_V, \quad (2)$$

Where $E_{G,HfAlO}$ and $E_{G,GaN}$ is the band-gap for HfAlO and GaN, respectively. With known values of the bandgap for HfO_2 (5.9 eV) and Al_2O_3 (7.0 eV), The bandgap of HfAlO (10 % Al_2O_3) estimated to be 6.0 eV using a linear interpolate.[16,39] Using a value of 6.0 eV for the HfAlO band-gap and a value of 3.4 eV for the GaN bandgap, a conduction band offset ΔE_C of 2.22 eV is obtained for the control sample.[40] Similarly, the valence band offset ΔE_V and conduction band offset ΔE_C for the HfAlO/GaN interface sample with *in situ* SiH_4 passivation are calculated to be 0.51 and 2.09 eV, respectively. The conduction band offset ΔE_C was lowered by amount of 0.13 eV for the sample with *in situ* SiH_4 passivation. Using the calculated values, the energy band diagram for the control and passivated samples can be deduced and are shown in Figure 3. From Figure 3, it can be seen that HfAlO/GaN interface has a Type I alignment for both samples. Also, the HfAlO/GaN interface with *in situ* SiH_4 passivation has a lower ΔE_C, compared to that of the control. Table 1 summarizes the differences between the core-levels as well as the valence and conduction band offsets obtained for the control and sample with *in situ* SiH_4 passivation.

The mechanism causing the difference in the band alignment at the HfAlO/GaN interface between the control sample and the sample with *in situ* SiH_4 passivation was revealed as the different ILs formed at the HfAlO/GaN interface. The effect of *in situ*

SiH_4 passivation on the band alignment at the HfAlO/GaN interface was then investigated. Figure 4 (a) shows the presence of GaO_x at the HfAlO/GaN interface for the control. With *in situ* SiH_4 passivation on GaN surface, the GaO_x disappears and a SiO_y is observed in Figure 4 (b). This signifies the presence of SiO_y, in place of GaO_x at the HfAlO/GaN interface. During the SiH_4 treatment, several monolayers of Si will be deposited on the GaN surface. For the GaN layer with *in situ* SiH_4 passivation prior to HfAlO deposition, the Ga-ON peak is absent as the GaN surface is protected by several monolayers of Si during the HfAlO deposition. Through XPS analysis, as shown in Figure 4 (b), these Si monolayers were subsequently oxidized (~1 nm SiO_y) during the HfAlO deposition [Figure 1 (b)]. It should be noted that Si was not introduced in the control sample, and oxidation of GaN surface took place during HfAlO deposition, thus lead to GaO_x IL formation in the control sample." As shown in Figure 5 (a), there is no obvious shift of the core-level Hf 4f peak for both samples, which means the band alignment difference for the samples with and without *in situ* SiH_4 passivation is not caused by the energy level change of the HfAlO layer. However, the peak of the core-level Ga 2p for the passivated sample shown in Figure 5 (b) was shifted to lower binding energy, as compared to the control, which indicates that the charges or the dipoles mainly reside at the IL/GaN interface. The peak shift (~ 0.24 eV) of the core-lelvel Ga 2p for the passivated sample is due to the chemical shift or the removal of native oxide at interface layer. With The band alignment difference, such as 0.13 eV ΔE_C difference, is mainly caused by the chemical shift or core-level up-shift in the GaN.[25] With GaO_x IL layer being replaced by SiO_y IL layer at GaN/HfAlO interface, there is an upward energy band bending towards IL/HfAlO interface.[25] It was reported that the interface traps located at

HfAlO/GaN interface could also contribute to band alignment difference, but the effect of interface trap could not account for 0.13 eV difference in ΔE_C.[41] Therefore, the band alignment for HfAlO/GaN interface is dominated by the chemical bonding of IL, which further leads to up-shift of core level of GaN layer.

4. Conclusion

In conclusion, the band alignment of MOCVD-HfAlO/GaN with different surface treatments was studied by high resolution XPS measurement. The valence band offset and corresponding conduction band offset for the HfAlO/GaN interface were found to be 0.38 eV and 2.22 eV, respectively, for the non-passivated sample, and 0.51 eV and 2.09 eV, respectively, for the sample with *in situ* SiH_4 passivation. The band alignment difference is believed to be dominated by the up-shift in the core level or chemical shift in the GaN substrate as a result of different interfacial layer formed by two different surface treatments. The physics details of the band alignment at HfAlO/GaN interface will provide a guide for the device design for AlGaN/GaN MOS-HEMTs with a thin GaN cap layer.

Acknowledgement. The authors would like to acknowledge the financial support from National Natural Science Foundation of China (Nos. 51371120, 51302174, and 61306126), the Science and Technology Foundation of Shenzhen, Science and Technology Commission of Shanghai Municipality (project number: 12ZR1453000), CAS International Collaboration and Innovation Program on High Mobility Materials

Engineering, and the Agency for Science, Technology and Research (A*STAR) (SERC1021500058) and Grant No. 1021690128) Singapore.

References

[1] C. Z. Lu, X. S. Xie, X. D. Zhu, D. F. Wang, A. Khan, I. Diagne, and S. N. Mohammad, J. Appl. Phys. 100 (2006) 113729.

[2] B. Monemar, J. Mater. Sci: Mater Electron 10 (1999) 227-254.

[3] Y.-F. Wu, B. P. Keller, S. Keller, D. Kapolnek, P. Kozodoy, S. P. Denbaars, and U. K. Mishra, Appl. Phys. Lett. 69 (1996) 1438-1440.

[4] G. Meneghesso, F. Rampazzo, P. Kordos, G. Verzellesi, and E. Zanoni, IEEE Trans. Electron Devices 53 (2006) 2932-2941.

[5] Y.-F. Wu, A. Saxler, M. Moore, R. P. Smith, S. Sheppard, P. M. Chavarkar, T. Wisleder, U. K. Mishra, P. Parikh, IEEE Electron Device Lett. 25 (2004) 117-119.

[6] R. Therrien, S. Singhal, J. W. Johnson, W. Nagy, R. Borges, A. Chaudhari, A. W. Hanson, A. Edwards, J. Marquart, P. Rajagopal, and K. L. Linthicum, IEDM 2005 Tech. Dig., (2005) 577-580.

[7] S. C. Binari, P. B. Klein, and T. E. Kazior, Proc. IEEE 9 (2002) 1048-1058.

[8] M.-W. Ha, Y.-H. Choi, J. Lim, and M.-K. Han, Jpn. J. Appl. Phys. 46 (2007) 2291-2295.

[9] N. Maeda, M. Hiroki, N. Watanabe, Y. Oda, H. Yokoyama, T. Yagi, T. Makimoto, T. Enoki, and T. Kobayashi, Jpn. J. Appl. Phys. 46 (2007) 547-551.

[10] C. T. Lee, Y. L. Chiou, and C. S. Lee, IEEE Electron Device Lett. (31) 2010 1220-1223.

[11] X. Z. Dang, R. J. Welty, D. Qiao, P. M. Asbeck, S. S. Lau, E. T. Yu, K. S. Boutros, and J. M. Redwing, Electron. Lett. 35 (1999) 602-603.

[12] E. Waki, T. Deguchi, A. Nakagawa, and T. Egawa, Appl. Phys. Lett. 92 (2008) 103507.

[13] R. Mehandru, B. Luo, J. Kim, F. Ren, B. P. Gila, A. H. Onstine, C. R. Abernathy, S. J. Pearton, D. Gotthold, R. Birkhahn, B. Peres, R. Fitch, J. Gillespie, T. Jenkins, J. Sewell, D. Via, and A. Crespo, Appl. Phys. Lett. 82 (2003) 2530-2532.

[14] T. Kikkawa, M. Nagahara, N. Okamoto, Y. Tateno, Y. Yamaguchi, N. Hara, K. Joshin, and P. M. Asbeck, IEDM 2001 Tech. Dig., (2001) 585-588.

[15] R. Mehandru, B. Luo, J. Kim, F. Ren, B. P. Gila, A. H. Onstine, C. R. Abernathy, S. J. Pearton, D. Gotthold, R. Birkhahn, B. Peres, R. Fitch, J. Gillespie, T. Jenkins, J. Sewell, D. Via, and A. Crespo, Appl. Phys. Lett. 82 (2003) 2530-2532.

[16] C. Liu, E. F. Chor, and L. S. Tan, Appl. Phys. Lett. 88 (2006) 173504.

[17] Y. C. Chang, H. C. Chiu, Y. J. Lee, M. L. Huang, K. Y. Lee, M. Hong, Y. N. Chiu, J. Kwo, and Y. H. Wang, Appl. Phys. Lett. 90 (2007) 232904.

[18] Z. H. Liu, G. I. Ng, S. Arulkumaran, Y. K. T. Maung, K. L. Teo, S. C. Foo, V. Sahmuganathan, T. Xu and C. H. Lee, IEEE Electron Device Lett. 31(2010) 96-98.

[19] P. D. Ye, B. Yang, K. K. Ng, J. Bude, G. D. Wilk, S. Halder, and J. C. M. Hwang, Appl. Phys. Lett. 86 (2005) 063501-3.

[20] J. Kim, B. Gila, R. Mehandru, J. W. Johnson, J. H. Shin, K. P. Lee, B. Luo, A. Onstine, C. R. Abernathy, S. J. Pearton, and F. Ren, J. Electrochemical Society 149 (2002) G482-G484.

[21] K. Balachander, S. Arulkumaran, H. Ishikawa, K. Baskar, and T. Egawa, Phys. Stat. Soli. (a) 202 (2005) R16-R18.

[22] M. S. Joo, B. J. Cho, C. C. Yeo, D. S. H. Chan, S. J. Whoang, S. Mathew, L. K. Bera, N. Balasubramanian, and D.-L. Kwong, IEEE Trans. Electron Devices 50 (2003) 2088-2094.

[23] Y. C. Chang, W. H. Chang, H. C. Chiu, L. T. Tung, C. H. Lee, K. H. Shiu, M. Hong, J. Kwo, J. M. Hong, and C. C. Tsai, Appl. Phys. Lett. 93 (2008) 053504.

[24] S. Y. Chiam, W. K. Chim, Y. Ren, C. Pi, J. S. Pan, A. C. H. Huan, S. J. Wang, and J. Zhang, J. Appl. Phys. 104 (2008) 063714.

[25] M. R. Coan, J. H. Woo, D. Johnson, I. R. Gatabi, and H.R. Harris, J. Appl. Phys. 112 (2012) 024508.

[26] X. Liu, E. K. F. Low, J. S. Pan, W. Liu, K. L. Teo, L. S. Tan, and Y.-C. Yeo, Appl. Phys. Lett. 99 (2011) 093504.

[27] Y.-L. Chiou, C.-S. Lee, and C.-T. Lee, Appl. Phys. Lett. (97) 2010 032107.

[28] X. Liu, H.-C. Chin, L. S. Tan, and Y.-C. Yeo, IEEE Trans. Electron Devices 58 (2011) 95-102.

[29] J. R. Waldrop and R. W. Grant, Appl. Phys. Lett. 68 (1996) 2879-2881.

[30] L. W.-W. Fang, J. S. Pan, R. Zhao, L. Shi, T.-C. Chong, G. Samudra, and Y.-C. Yeo, Appl. Phys. Lett. 92 (2008) 032107.

[31] E. T. Yu, E. T. Croke, D. H. Chow, D. A. Collins, M. C. Phullips, T. C. McGill, J. O. McCaldin, and R. H. Miles, J. Vac. Sci. Technol. B8 (1990) 908-915.

[32] E. A. Kraut, R. W. Grant, J. R. Waldrop, and S. P. Kowalczyk, Phys. Rev. Lett. 44 (1980) 1620-1623.

[33] M. Yang, L. Zhu, Y. Li, L. Cao, and Y. Guo, J. Alloys Com. 578 (2013) 143-147.

[34] H. H. Wei, G. He, X. S. Chen, J. B. Cui, M. Zhang, H. S. Chen, Z. Q. Sun, J. Alloys Com. 591 (2014) 240-246.

[35] Y. Yang, C. G. Jin, Z. F. Wu, X. M. Wu, L. J. Zhuge, T. Yu, J. Alloys Com. 605 (2014) 68-72.

[36] Y.-L. Chiou and C.-T. Lee, IEEE IEEE Trans. Electron Devices 58 (2011) 3869-3875.

[37] J. J. Chen, B. P. Gila, M. Hlad, A. Gerger, F. Ren, C. R. Abernathy, and S. J. Pearton, Appl. Phys. Lett. 88 (2006) 142115.

[38] P. D. C. King, T. D. Veal, C. E. Kendrick, L. R. Bailey, S. M. Durbin, and C. F. McConville, Phys. Rev. B, Condens. Matter. 78 (2008) 033308.

[39] M. V. Hove, S. Boulay, S. R. Bahl, S. Stoffels, X. Kang, D. Welleken, K. Greens, A. Delabie, and S. Decoutere, IEEE Electron Device Lett. 33 (2012) 667-669.

[40] B. Gelmont, K. Kim, and M. Shur, J. Appl. Phys. 74 (1993) 1818-1821.

[41] M. H. S. Owen, M. A. Bhuiyan, Q. Zhou, Z. Zhang, J. S. Pan, and Y.-Y. Yeo, Appl. Phys. Lett. 104 (2014) 091605.

Figures Caption

Fig.1 (a) Cross-sectional TEM images of HfAlO/GaN sample without *in situ* SiH_4 passivation, showing that a native oxide interfacial layer (~ 1 nm) was formed on the GaN surface. (b) Cross-sectional TEM images of HfAlO/GaN sample with *in situ* SiH_4 passivation, showing that an oxidizing Si layer (~ 1 nm) was formed on the GaN surface.

Fig. 2 The core-level and valence band spectra for (a) bulk GaN and (b) bulk HfAlO samples. The intercept between the base line and the slope of the leading edge gives the valence band maximum VBM of the sample, where the Fermi level is taken as the reference level. The core level spectra of Ga 3p and Hf 4f obtained for (c) control and (d) *in situ* SiH_4 passivated HfAlO(3nm)/GaN interface sample are also obtained. Energy differences between core level and VBM are computed as shown for the subsequent calculation of ΔE_V.

Fig.3 (a) Schematic of energy band line-up at the HfAlO/GaN heterointerface without *in situ* VA anneal and SiH_4 treatment. (b) Schematic of energy band line-up at the HfAlO/GaN heterointerface with *in situ* VA anneal and SiH_4 treatment. Energy band line-up for HfAlO/GaN interface with and without *in situ* VA anneal and SiH_4 treatment has a Type I alignment. Numerical values of ΔE_C, ΔE_V, and ΔE_{CL} obtained using XPS are also indicated.

Fig. 4 XPS showing the Ga 3p spectra of two GaN samples coated with ~ 3 nm HfAlO. (a) Ga-O peaks are observed for the sample without *in situ* VA anneal and SiH_4 treatment, and (b) Ga-O peak disappears for the sample with *in situ* VA anneal and SiH_4 treatment, and Si-O peak is detected.

Fig. 5 XPS shows the core levels of (a) Hf 4f and (b) Ga 2p spectra for two samples shown in Fig. 4. With *in situ* VA anneal and SiH_4 treatment, the binding energy (BE) of Ga 2p peak is shifted to lower BE, as compared with that of control sample. The change in the band alignment is mainly due to the up-shift in the core level in the GaN.

Table Caption

Table 1: Differences between the core-levels as well as the valence and conduction band offsets obtained for the control and sample with *in situ* SiH_4 passivation.

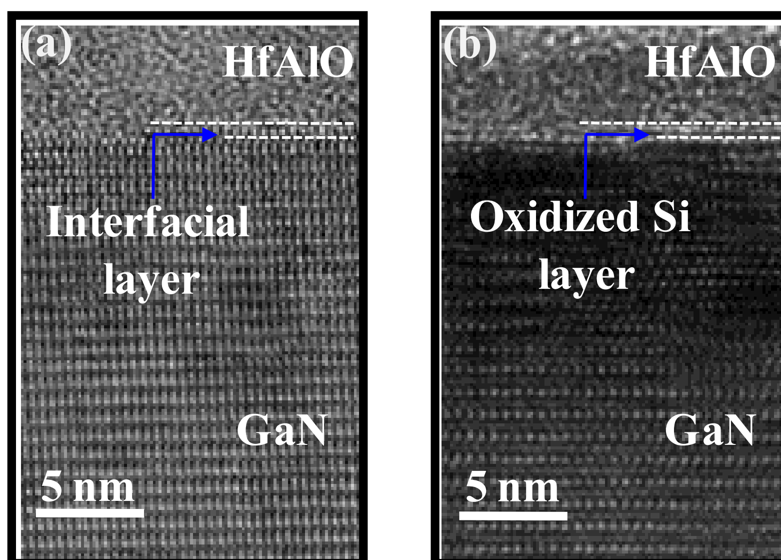

Figure 1. Liu *et al.*

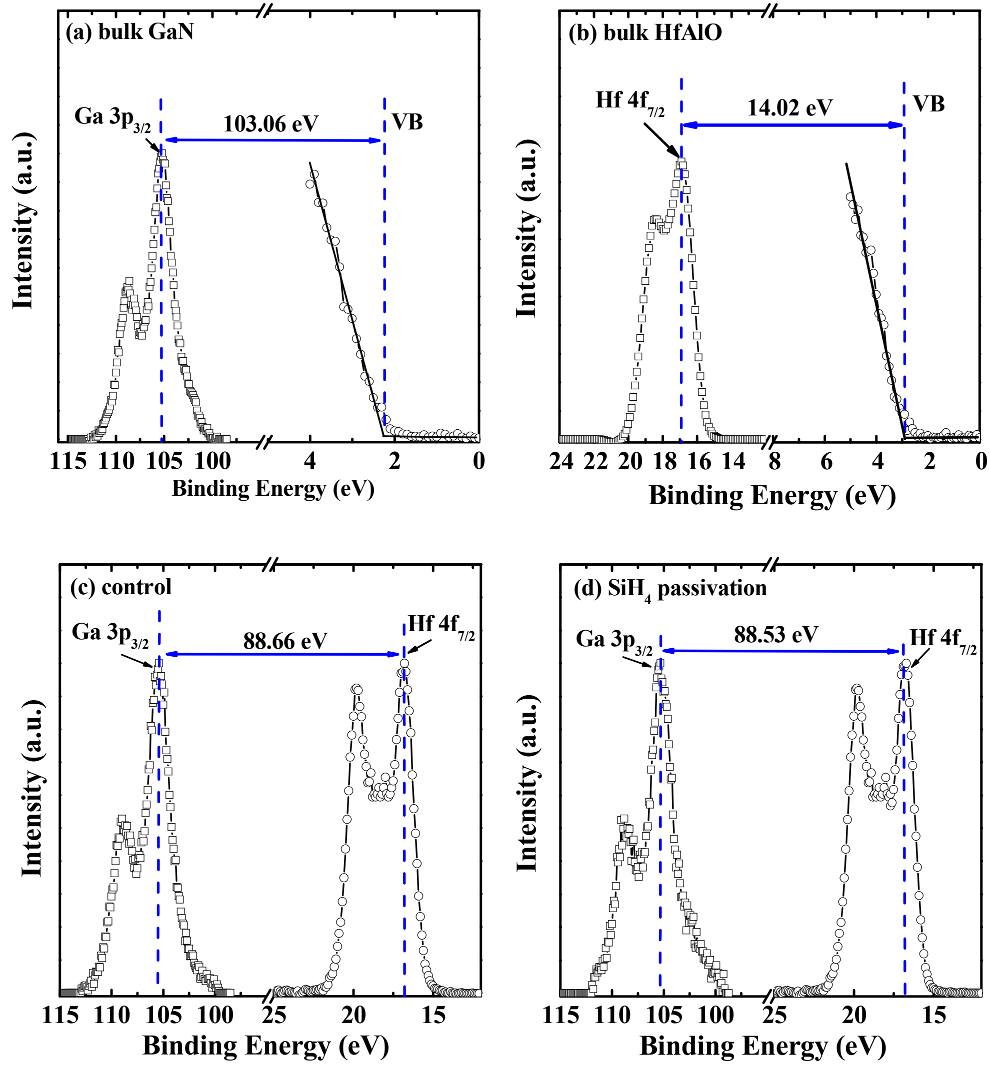

Figure 2. Liu *et al.*

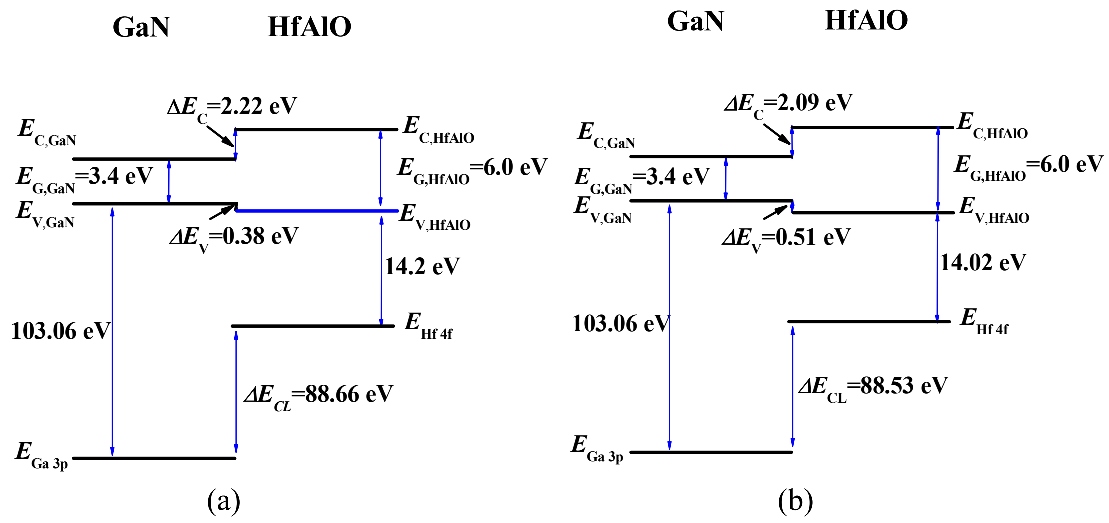

Figure 3. Liu *et al.*

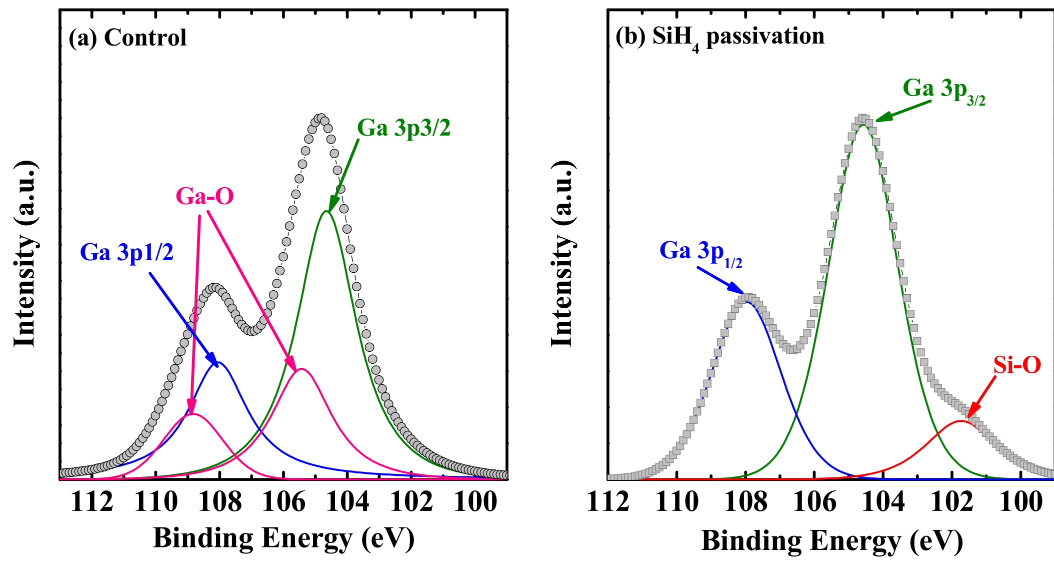

Figure 4. Liu *et al.*

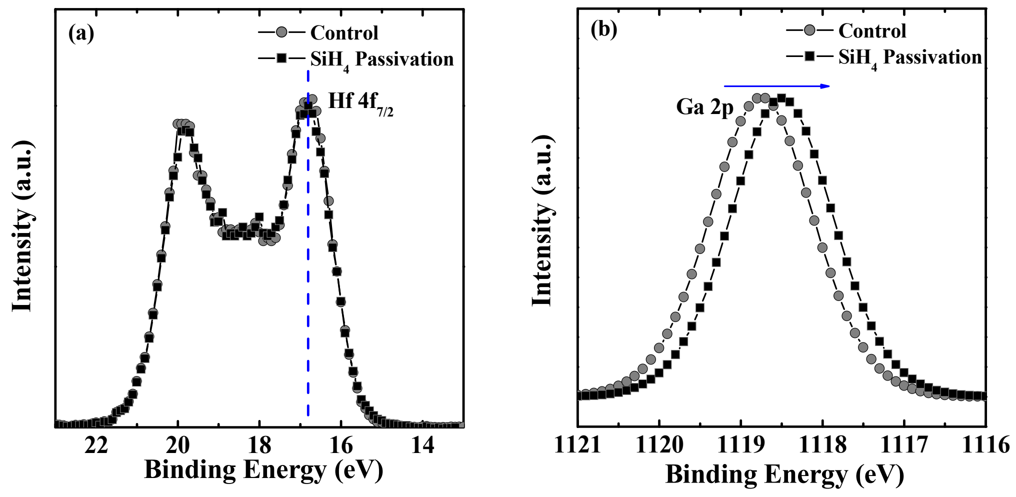

Figure 5. Liu *et al.*

Band parameters	**Control**	**SiH_4 passivation**
ΔE_{CL}	88.66 eV	88.53 eV
ΔE_C	2.22 eV	2.09 eV
ΔE_V	0.38 eV	0.51 eV

Table 1. Liu *et al.*